ELSEVIER

Chemical Engineering Journal 85 (2002) 27–34

Chemical Engineering Journal

www.elsevier.com/locate/cej

Stability of latex crossflow filtration: cake properties and critical conditions of deposition

G. Gésan-Guiziou [a,*], R.J. Wakeman [b], G. Daufin [a]

[a] *Laboratoire de Recherches de Technologie Laitière, INRA, 65 rue de Saint Brieuc, 35042 Rennes cedex, France*
[b] *Department of Chemical Engineering, Loughborough University, Loughborough LE11 3TU, Leicestershire, UK*

Received 30 June 2000; received in revised form 17 February 2001; accepted 19 February 2001

Abstract

The critical permeation flux is the flux at which cake deposition starts to be detectable. The variations of the critical flux (determined simultaneously by a mass balance and successive variations of transmembrane pressures) during sub-micron latex particles filtration were studied under various operating conditions (membrane pore diameter, shear stress at the membrane surface, latex concentration, surfactant content). These variations were explained taking into account the properties of the suspension and of the fouling deposit (reversibility, specific resistance, thickness, porosity) formed beyond the critical threshold. It was shown that the critical parameter, J_{crit}/τ_w, which defines the conditions required for stable filtration performance was more appropriate than $\Delta P_{crit}/\tau_w$ previously suggested in the literature since J_{crit} was actually independent of the clean hydraulic resistance of the membrane, and consequently of the membrane pore size. This indicates that there is no need to work with the largest pore size membrane: larger pores will not induce higher critical flux and will not improve the area of the stability zone of the filtration. This work also points out the major impact of surfactants on fouling phenomena and J_{crit}, observations rarely reported in the literature: the higher the surfactant content, the higher the deposited mass and the lower J_{crit}.

Keywords: Crossflow filtration; Critical permeation flux; Latex; Fouling; Deposition

1. Introduction

In crossflow filtration, membrane fouling mechanisms involving colloids are still not satisfactorily explained, although numerous studies have been dedicated to this problem. Different works lead to the conclusion that there exists a critical permeation flux, J_{crit}, below which there is no marked fouling by colloidal particles, and above which particles deposit and filtration performances are altered (sharp increase of fouling, reduced operating time, large decrease in permeability and solute transmission) [1–3]. The deposition of latex and yeast above the critical flux have recently been observed by a microscope coupled with a video camera [4]. However, few proposals have been advanced for the prediction of J_{crit} under various operating conditions, and experimental works have generally been restricted to conditions not commonly found in practical applications: dead-end filtration [5], low shear rate [6,7], low particle concentration [6]. Moreover, few studies have reported the relationships between deposit characteristics formed above the critical flux and critical flux values.

This work is intended to study the variations of J_{crit} in the case of sub-micron particles under various operating conditions (shear stress at the membrane surface, pore diameter, latex concentration, surfactant content) within the ultra- and micro-filtration range and to explain these evolutions using the properties of the deposit (hydraulic resistance, reversibility, thickness, porosity) formed beyond the critical threshold. Such information are necessary for better understanding crossflow filtration stability and reasons of filtration alterations.

2. Experimental

2.1. Latex suspension

A suspension of latex stabilised by surfactants was used. The average diameter of the latex particles (d_p) (Mastersizer S, Ver. 2.18, Malvern Instruments) was 190 nm with a narrow size distribution: the 10 and 90 vol.% sizes were 80 and 400 nm, respectively. In the calculations the polydispersity

* Corresponding author. Tel.: +33-2-23-48-53-25; fax: +33-2-23-48-53-50.
E-mail address: gesan@labtechno.roazhon.inra.fr (G. Gésan-Guiziou).

1385-8947/02/$ – see front matter
PII: S1385-8947(01)00149-8

Nomenclature

A	membrane area (m^2)
C_{latex}	concentration of latex particles ($g\,kg^{-1}$)
d_p	average diameter of the latex particles (m)
f	Fanning friction factor (–)
J	permeation flux ($m\,s^{-1}$ or $l\,h^{-1}\,m^{-2}$)
J_{crit}	critical permeation flux ($m\,s^{-1}$ or $l\,h^{-1}\,m^{-2}$)
J_{lim}	limiting permeation flux ($m\,s^{-1}$ or $l\,h^{-1}\,m^{-2}$)
J_w	initial permeation flux of water ($m\,s^{-1}$ or $l\,h^{-1}\,m^{-2}$)
$J_{w'}$	final permeation flux of water ($m\,s^{-1}$ or $l\,h^{-1}\,m^{-2}$)
M_d	deposited mass of latex ($kg\,m^{-2}$)
ΔP	transmembrane pressure (Pa or bar)
R_a	hydraulic resistance due to surfactant adsorption (m^{-1})
R_{dep}	hydraulic resistance due to deposition (m^{-1})
R_{if}	irreversible fouling hydraulic resistance (m^{-1})
R_m	cleaned membrane hydraulic resistance (m^{-1})
$R_{m'}$	initial hydraulic resistance of irreversibly fouled membrane (m^{-1})
Re	Reynolds number (–)
s	compressibility of the cake layer (–)
t	time (s or min)
v	mean tangential flow velocity ($m\,s^{-1}$)

Greek symbols

α	specific resistance of the cake layer ($m\,kg^{-1}$)
δ	thickness of the cake layer (m)
ε	porosity of the cake layer (–)
μ	dynamic viscosity of latex suspension (Pa s)
μ_w	dynamic viscosity of water (Pa s)
ρ_r	density of the retentate ($m^3\,kg^{-1}$)
ρ_s	density of the latex particle ($m^3\,kg^{-1}$)
τ_w	shear stress at the membrane wall (Pa)

of the particle size was neglected. At pH 7.0, the zeta potential values of the particles (ZetaMaster, Ver. 1.27, Malvern Instruments) ranged from −40 to −63 mV according to ionic strength (from 5×10^{-5} to 0.2 M adjusted with NaCl) (Fig. 1). Zeta potential was calculated from electrophoretic mobility using Henry's law, and corrected according to O'Brien and White [8] as suggested by Harmant and Aimar [9]. Fig. 1 shows a decrease of zeta potential as the electrolyte concentration approached a given value, called the critical coagulation concentration. At this value, particle diameter tends to increase. The critical coagulation concentration was estimated to be around 0.1 M for sodium chloride, which is similar to the value obtained by Harmant and Aimar [9].

During the 5–6 h filtration experiments, the latex suspension was stable (constant average size (190 ± 10 nm) and zeta potential (−47 ± 4 mV)), indicating that the aggregation phenomenon was avoided.

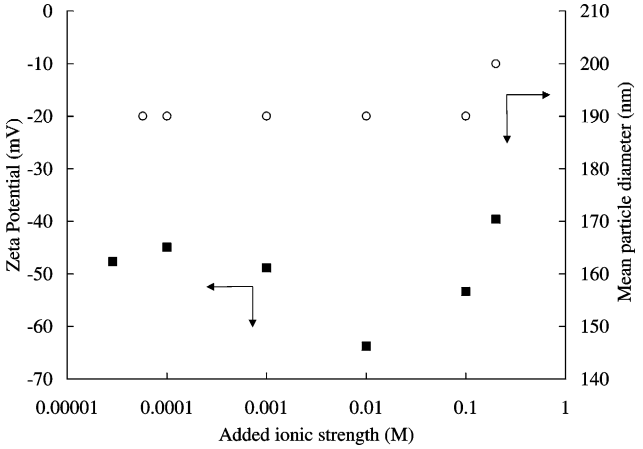

Fig. 1. Zeta potential and mean particle diameter of latex suspension versus added ionic strength (pH 7.0 adjusted with HCl, 0.05 M; $C_{latex} = 0.1\,g\,kg^{-1}$).

The particle density (ρ_s) was estimated to 1000 ± 10 $kg\,m^{-3}$ by measuring the mass of a given volume of known mass concentration. Whatever the latex concentration, C_{latex} in the range 0–340 $g\,kg^{-1}$, the suspension behaviour was Newtonian (CS-100 Rheometer, TA Instruments). The viscosity, μ was 1.00 ± 0.05 mPa s^{-1} up to a concentration of 10 $g\,kg^{-1}$ and then increased exponentially with latex concentration according to:

$$\mu = 0.95 \times 10^{-3} \exp(0.0045 C_{latex}) \quad (1)$$

where μ in Pa s and C_{latex} in $g\,kg^{-1}$.

The decrease in the surfactant content of latex suspension (decrease of suspension conductivity by 40%) was achieved by diafiltration of a concentrated suspensions with double distilled water (3 μS cm^{-1} in conductivity). The increase in surfactant was performed by diluting the initial latex suspension with the diafiltration permeate.

2.2. Experimental set-up and operating conditions

The study was carried out using an experimental set-up previously described in detail [10]. The unit comprised a flow circuit (total volume of 5.2 l), in which suspension of a known concentration was pumped continuously through a crossflow filtration membrane. All the experiments were conducted at v ranging from 0.5 to 1.5 $m\,s^{-1}$ (±10%) and ΔP from 0.0×10^5 to 1.6×10^5 Pa (±15%) at a constant temperature of 50 ± 2 °C and pH 7. The values of v corresponded to a Reynolds number, Re ranging from 3,780 to 11,350 at 50 °C (that is to say in turbulent regime), and a wall shear stress, τ_w ranging from 1.2 to 6.5 Pa. The wall shear stress, τ_w is the force exerted by a fluid flowing tangentially to the membrane on an element of its surface area. Because the small longitudinal pressure drop did not allow us to measure it directly, τ_w was calculated from:

$$\tau_w = \tfrac{1}{2} f \rho_r v^2 \quad (2)$$

where f is the Fanning friction factor, ρ_r the density of the suspension in the retentate side and v the mean crossflow velocity. Under turbulent flow conditions and for Newtonian fluids, the friction factor can be calculated using the approximation of Blasius, assuming the membrane to be a smooth tubular element [3]:

$$f = 0.08\,Re^{-0.25} \tag{3}$$

where Re is the Reynolds number.

2.3. Membranes

The ultrafiltration membranes used were tubular ceramic Kerasep membranes (15 and 300 kg mol^{-1} cut-off, 0.60 m long, seven channels of 4.5 mm inner diameter) provided by Orelis (01 Miribel, France). The selected cut-offs implied no (15 kg mol^{-1}) or negligible internal fouling or pore blocking (300 kg mol^{-1}). Permeability of these membranes was measured at $50 \pm 2\,^{\circ}$C before the experiment from the distilled water fluxes, J_w using Darcy's law:

$$J_w = \frac{\Delta P}{\mu_w R_m} \tag{4}$$

where μ_w is the dynamic viscosity of water.

Tubular ceramic Kerasep membranes with 0.1 μm mean pore diameter (0.6 m long, seven channels of 4.5 mm inner diameter, from Orelis, France) were fouled prior to the experiment using latex suspension. The large amount of fouling obtained was mainly due to irreversible pore bloking with latex particles (sharp hysteresis of deposited mass, see Section 2.4.2).This irreversible fouling was uncleanable and allowed experiments to be performed using membranes with initial hydraulic resistances, $R_{m'}$ ranging from 7.3 to 20.9×10^{11} m^{-1} (values higher than the hydraulic resistance of the clean membrane, R_m). High $R_{m'}$ were obtained after successive experiments performed at high crossflow velocities and high latex concentrations.

2.4. Experimental procedure

Prior to the start of a filtration experiment, the process suspension prepared by dilution of the initial suspension with doubled distilled water (3 μS cm^{-1} in conductivity) was stirred in the feed tank for 5 min to produce an homogeneous suspension throughout the retentate compartment. The pH 7 was then adjusted with 0.05 M HCl. The volume reduction ratio was constant and equal to 1 since the filtrate produced was continuously returned to the feed tank via a flowmeter.

2.4.1. Determination of critical flux

J_{crit} is the critical flux above which particles start to accumulate. It was determined by successive variations of transmembrane pressure (step by step technique) and by mass balance of retained latex particles.

The *step by step technique* consisted in systematic increase of ΔP (30 min at each ΔP step before J_{crit} was reached, 15 min afterwards) [3]; the first unstable permeation flux was determined when J decreased over the course of the time (Fig. 2a), leading to a non-linearity in the $J = f(\Delta P)$ relationship (Fig. 2c). At this point, the deposited mass, estimated by mass balance became positive (see Section 2.4.2 and Fig. 2b) and the hydraulic resistance due to deposition, R_{dep} increased significantly (Fig. 2b). When $J = f(\Delta P)$ was linear and similar to values obtained with water, R_{dep} was defined according to Darcy's law as:

$$J = \frac{\Delta P}{\mu_p (R_m + R_{dep})} \tag{5}$$

where μ_p is the dynamic viscosity of permeate similar to μ_w.

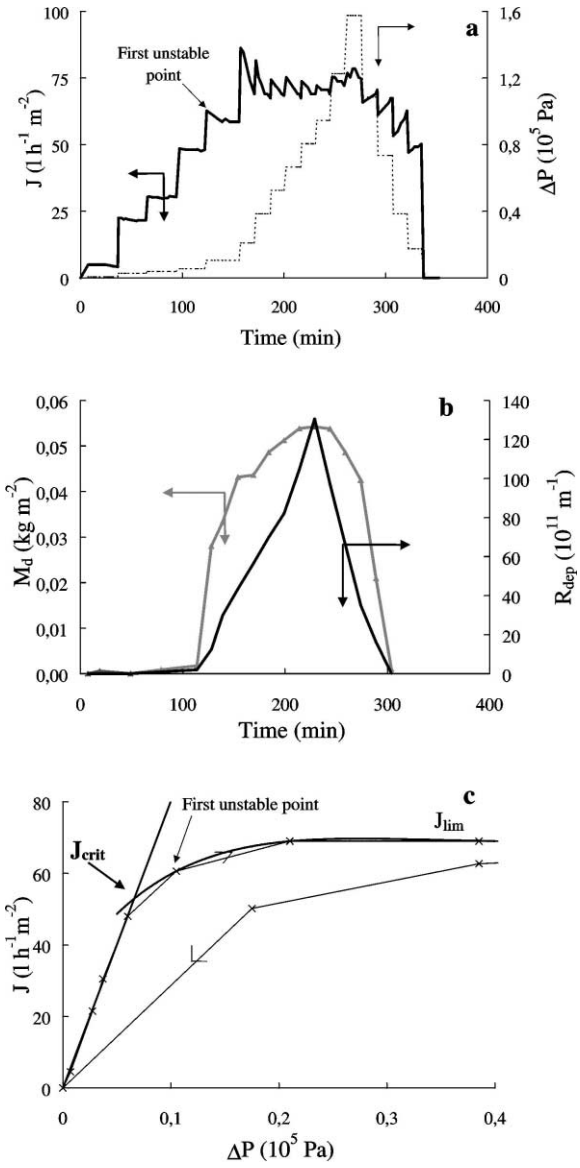

Fig. 2. Determination of the critical permeation flux. (a) Permeation flux, J and transmembrane pressure, ΔP versus time. (b) Deposited mass of latex, M_d and hydraulic resistance due to deposition, R_{dep} versus time. (c) Permeation flux, J versus transmembrane pressure, ΔP. Conditions: membrane 300 kg mol^{-1}; $C_{latex} = 1.74$ g kg^{-1}; $\tau_w = 1.2$ Pa ($v = 0.5$ m s^{-1}); $T = 50\,^{\circ}$C.

When $J = f(\Delta P)$ was linear but lower than the values obtained with water, R_{dep} was defined as:

$$J = \frac{\Delta P}{\mu_p(R_m + R_a + R_{dep})} \quad (6)$$

where R_a is the hydraulic resistance due to surfactant adsorption easily determined with the slope of $J = f(\Delta P)$ linear relationship during latex filtration.

The critical values of transmembrane pressure and permeation flux (ΔP_{crit}; J_{crit}) were experimentally determined by the intercept of the linear relationship $J = f(\Delta P)$ when $J < J_{crit}$ (J stable in the course of the time; no deposited latex) and of a polynomial fitting when $J > J_{crit}$ (decrease of J; increase of deposited mass) (Fig. 2c). The error of the determination of J_{crit} was estimated to be $\pm 5\,l\,h^{-1}\,m^{-2}$.

For some operating conditions, the determination of J_{crit} was confirmed by experiments performed in the course of time: the evolution of the permeation flux J at constant ΔP at a permeation flux below J_{crit} and at a J value marginally beyond the critical value were followed for 5 h.

2.4.2. Determination of the properties of the cake layer

Reversibility. Reversibility of the cake-layer was studied by cyclical experiments: ΔP was decreased after being previously increased up to 1.6×10^5 Pa (largely higher than ΔP_{crit} whatever the operating conditions used), and J recorded. The presence of a hysteresis in $J = f(\Delta P)$ (Fig. 2c) indicates that some irreversible deposition occurred. The irreversible fouling hydraulic resistance, R_{if} was determined by measuring the permeability of the membrane at $50 \pm 2\,^{\circ}C$ after the experiment from the distilled water fluxes ($J_{w'}$) using Darcy's law:

$$J_{w'} = \frac{\Delta P}{\mu_w(R_m + R_{if})} \quad (7)$$

R_{if} is the hydraulic resistance that remains after the water rinsing of the membrane. It takes into account both the surfactant adsorption phenomena and irreversibility of deposit structure.

Deposited mass, M_d ($kg\,m^{-2}$). During the experiments, the latex concentration was deduced from turbidity measurements (Turbidimeter Hach Company, Loveland, USA), using a calibration curve. Retentate and permeate samples were withdrawn every 15 min. Circulating the suspension in the filtration loop without permeation revealed a constant bulk concentration indicating that no significant adhesion or adsorption of latex occurred. As the permeate was continuously recycled and contained no latex particles, any decrease in bulk concentration corresponded to a deposition of particles at the membrane surface. The deposited mass is calculated from a mass balance as the difference between the initial mass from which the mass of samples withdrawn was subtracted and mass measured in the retentate. The bulk concentration typically decreased by 20–60%, depending on the operating conditions, for a ratio membrane area/volume of suspension around $11\,m^2/m^3$. The upper error on the mass calculation was estimated to be 10%.

Specific resistance, α ($m\,kg^{-1}$). The specific resistance is calculated as follows:

$$R_{dep} = \alpha M_d \quad (8)$$

Compressibility, s. The evolution of α versus ΔP enable the compressibility, s to be calculated:

$$\alpha = B\Delta P^s \quad (B: \text{constant}) \quad (9)$$

Porosity, ε. Based on the Carman–Kozeny equation, the porosity (cake voidage) ε can be evaluated for spherical particles (Kozeny constant = 5) by:

$$\alpha = \frac{180(1-\varepsilon)}{\varepsilon^3 \rho_s {d_p}^2} \quad (10)$$

Thickness, δ. The thickness δ is expressed with the known deposited mass, M_d:

$$\delta = \frac{M_d}{\rho_s(1-\varepsilon)} \quad (11)$$

Experiments performed in the course of the time or by stepwise variations of ΔP showed similar deposit characteristics. Moreover, due to the small longitudinal pressure drop, deposit characteristics were assumed to be constant all along the filtering path.

Some filtration experiments were performed in duplicate with a good reproducibility (<5% for permeation flux and deposit characteristics).

3. Results

3.1. The critical permeation flux, J_{crit}

Whatever the operating parameters studied, the stepwise experiments showed two zones:

Below the critical flux, experiments performed over the course of the time showed that, J could be maintained as constant for several hours (5 h) and was similar to the flux measured with water at the same ΔP. Since no decrease in latex concentration in the feed tank was observed below J_{crit}, no cake formation was likely to occur and the filtration operated in a stable regime. According to Wu et al. [7] this definition of J_{crit} corresponds to the "strong form" of critical flux. At high latex concentrations, some deviations between the permeation flux and the water flux were, however, observed (≈15% at $C_{latex} = 7.7\,g\,kg^{-1}$). In such conditions, the final water flux ($J_{w'}$) was lower than the initial one (J_w), but since the relationship between transmembrane pressure and flux was linear and no decrease in latex concentration was detected in the feed tank, this deviation was assumed to be due to surfactant adsorption. In these conditions J_{crit} corresponds to the "weak form" of critical flux [7].

Above the critical threshold, R_{dep} increased indicating the conditions where cake formation occurred: the increase in

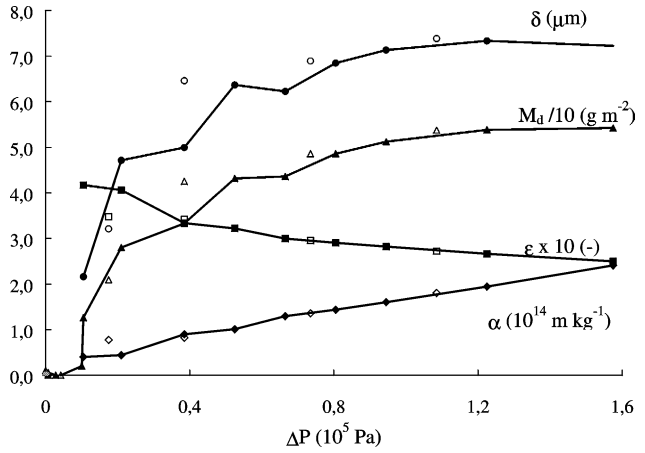

Fig. 3. Evolution of deposit characteristics (deposited mass, M_d; thickness, δ; porosity, ε and specific resistance, α of the deposit) during the successive increase (closed symbols and black lines) and decrease (open symbols) in transmembrane pressure, ΔP. Conditions: see Fig. 2.

R_{dep} was directly related to the increase in mass deposited at the membrane surface (sharp decrease in latex concentration in the feed tank) (Fig. 2b). Under a further increase in ΔP, J reached the limiting flux, J_{lim} (Fig. 2c), frequently reported with macromolecular solutions and colloidal suspensions. The deposited mass and thickness increased with ΔP until J_{lim} was reached, and decreased totally or partially when ΔP was released (Fig. 3).

The porosity of the deposit varied slightly with ΔP and ranged from 0.40 to 0.25 (Fig. 3), which is in accordance with values theoretically calculated for incompressible monodisperse particles [11]. Such a low porosity indicated a probable compression of the deposit and a high packing density, which agrees with published work on the visualisation of cake formation in crossflow filters [10]. The specific resistance was found to depend on ΔP ($2.6 \pm 0.8 \times 10^{10} \Delta P^{0.76\pm0.03}$ m kg^{-1}, ΔP in Pa).

3.2. Evolution of J_{crit} and deposit characteristics versus operating parameters

3.2.1. Wall shear stress, τ_w

The higher the wall shear stress, the lower the deposited mass and thickness, and the higher J_{crit} (Fig. 4). The specific resistance and the porosity were found to be independent of τ_w. The influence of τ_w on the filtration resistance was then mainly determined by the amount of deposit.

For a given latex concentration, J_{crit} increased linearly with τ_w (Fig. 4). The ratio of J_{crit}/τ_w was consequently constant and equal to 18 l h^{-1} m^{-2} Pa^{-1}.

3.2.2. Initial hydraulic resistance of the membrane

Whatever the hydraulic resistance of the clean membrane, R_m (and consequently pore size), J_{crit} and the deposit characteristics (deposited mass, porosity, thickness) were similar (Fig. 5a). J_{crit} was consequently independent of the initial hydraulic resistance of the clean membrane. However, when the initial hydraulic resistance of the membrane was changed as a result of irreversible fouling, $R_{m'}$, J_{crit} decreased sharply (Fig. 5b), leading to strong irreversible phenomena (sharp hysteresis $J = f(\Delta P)$, high R_{if}).

3.2.3. Concentration in latex

J_{crit} decreased and the deposited mass and deposit thickness increased with increasing latex concentrations up to 3 g kg^{-1} (Fig. 6). At a concentration higher than 3 g kg^{-1}, J_{crit} and the deposit characteristics remained nearly stable. The specific resistance and the porosity (0.25 ± 0.01) were found to be independent of solid concentration.

3.2.4. Concentration of surfactants

Fig. 7 shows that an increase in suspension conductivity of a given latex concentration (due to an increase in surfactant and ionic contents) led to a lower J_{crit} and higher deposited mass and deposit thickness. The porosity, however, did not

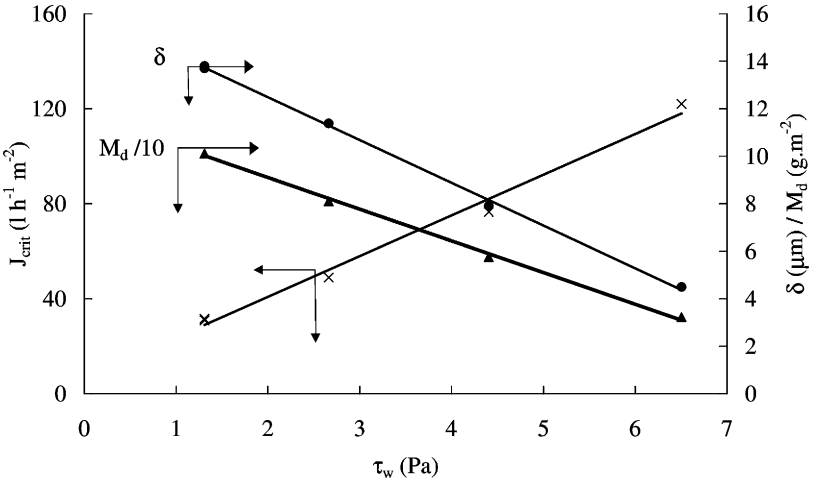

Fig. 4. Critical permeation flux, J_{crit} and deposit characteristics (deposited mass, M_d; deposit thickness, δ) versus wall shear stress, τ_w. Conditions: membrane 300 kg mol^{-1}; $C_{latex} = 4.9$ g kg^{-1}; $T = 50\,^{\circ}$C.

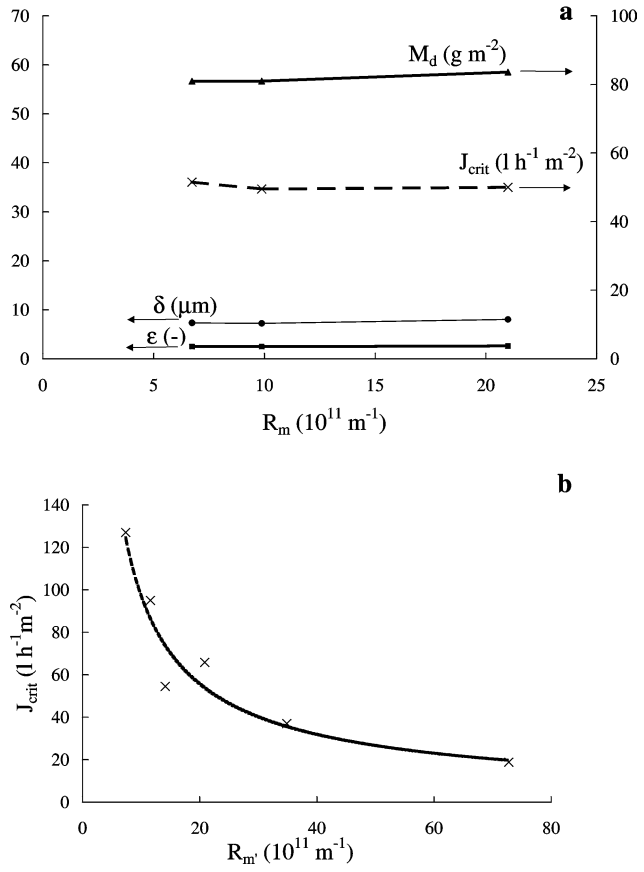

Fig. 5. Critical permeation flux, J_{crit} and deposit characteristics (deposited mass, M_d; thickness, δ and porosity, ε of the deposit) versus initial hydraulic resistance of: (a) clean membrane, R_m; conditions: 15 (1) and 300 kg mol^{-1} (two batches) membranes; $C_{latex} = 1.80$ g kg^{-1}; $\tau_w = 1.2$ Pa; $T = 50$ °C; (b) membrane with irreversible residual fouling, $R_{m'}$; conditions: membrane 300 kg mol^{-1}; $C_{latex} = 0.48$ g kg^{-1}; $\tau_w = 1.2$ Pa; $T = 50$ °C.

significantly depend on the surfactant and ionic contents of the suspension (Fig. 7). The higher the surfactant and ionic contents, the more pronounced the irreversible phenomena (hysteresis, R_{if}).

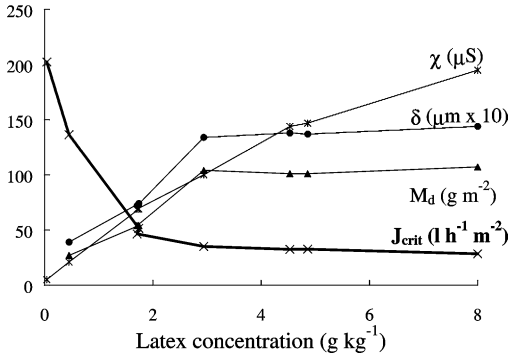

Fig. 6. Evolution of conductivity (χ) of the filtered latex suspension, of critical permeation flux, J_{crit} and deposit characteristics (deposited mass, M_d and thickness, δ of the deposit) versus latex concentration. Conditions: membrane 300 kg mol^{-1}; $\tau_w = 1.2$ Pa; $T = 50$ °C.

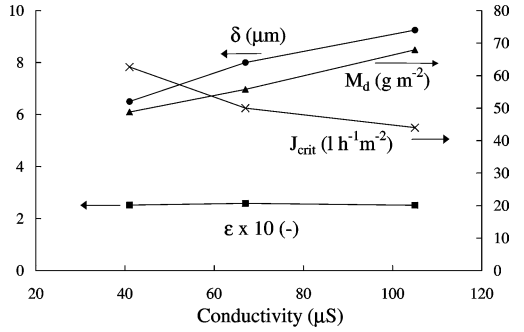

Fig. 7. Evolution of critical permeation flux, J_{crit} and deposit characteristics (deposited mass, M_d; thickness, δ and porosity, ε of the deposit) versus suspension conductivity. Conditions: membrane 300 kg mol^{-1}; $C_{latex} = 1.80$ g kg^{-1}; $\tau_w = 1.2$ Pa; $T = 50$ °C.

4. Discussion

The characteristics of latex particles deposit vary with crossflow filtration operating conditions (transmembrane pressure, permeation flux, wall shear stress, concentration of latex and surfactants) and they play a basic role in affecting the critical parameter, J_{crit}/τ_w, which defines the operating conditions required for high stable filtration performance.

4.1. Appropriate critical parameter

J_{crit}/τ_w can be considered as a critical parameter, since, for a given latex concentration, the critical permeation flux, J_{crit}, under which there is no deposit of latex, increased linearly with the wall shear stress. In micro-filtration (MF) of dairy products (containing "particles" such as casein micelles, aggregates, or bacteria to be retained), it has already been shown that J_{crit}/τ_w rules the performance of the separation (permeability and selectivity) [3]. The present study shows however that, for a given ratio J_{crit}/τ_w, the deposit characteristics were not similar: the higher the τ_w, the lower the deposited mass, although the porosity of the deposit was constant (presumably due to the low polydispersity of the latex suspension).

The parameter J_{crit}/τ_w is more appropriate than $\Delta P_{crit}/\tau_w$ previously proposed in the literature [10,12] because J_{crit} is independent of the initial hydraulic resistance of the clean membrane (or initial pore size of the membrane), in contrast with the transmembrane pressure. Previous works [7,13] have already studied the effect of membrane pore size on critical flux, but none of them compared the values of J_{crit} obtained with different membrane pore sizes under similar fouling conditions. Wu et al. [7] have observed a decrease in J_{crit} with increasing membrane pore size for each of the three tested fluids (bovine serum albumin solution, silica particles, yeast suspensions). According to the authors this could be due either to different charge effects and interactions as a result of different membrane materials or to changes in membrane porosity induced by internal fouling. Madaeni et al. [13] have shown that the critical flux is insensitive to

the pore size of the Millipore membranes, but in that work for a given permeation flux the largest pore size membranes were found to produce higher ΔP indicating that some pore blocking occurred.

For a given membrane separation, the independence of the critical parameter J_{crit}/τ_w from the membrane pore size indicates that there is no need to work with the largest pore size membrane: larger pores will not induce higher critical flux and will not improve the area of the stability zone of the filtration; however the risk of internal fouling would be greater. Smaller pores could, therefore, be preferred provided the transmembrane pressure required to get to J_{crit} remains lower than the longitudinal pressure drop in order not to induce an increase in energy consumption.

Considering the independence of J_{crit} from the membrane pore size, and since J_{crit} indicates the conditions where cake formation occurs, J_{crit} is to be considered as the outcome of the balance between the convective force exerted on the particles towards the membrane and back-transport such as erosion (which is greater at higher crossflow and wall shear stress). A higher critical flux at higher crossflow is, therefore, expected. The net accumulation of particles arises from an imbalance between convection towards the membrane and removal which is generally assumed to be proportional to the shear stress according to [14]:

$$A(JC_{latex} - a\tau_w) = \frac{dM_d}{dt} \quad (12)$$

where A is the membrane area and "a" an experimentally determined constant [14]. According to Eq. (12), at the critical flux, there is no accumulation ($dM_d/dt = 0$) and JC_{latex} ($=J_{crit}C_{latex}$) becomes, therefore, proportional to τ_w.

The evidence that "a" in Eq. (12) is constant is limited; for this to be so suggests that at a constant τ_w, $J_{crit}C_{latex}$ is a constant or that the ratio $(J_{crit}C_{latex})/\tau_w$ should remain constant, which is not observed experimentally. The experimental data, therefore, indicates that "a" is not a constant, but is a function of C, which means that the assumption to establish Eq. (12) is not valid in the present case.

With a complex feed such as the latex used in this study, the increase of the ratio $(J_{crit}C_{latex})/\tau_w$ with increasing latex concentration is due to stabilisation of the deposit characteristics, which may be induced by an increase in surfactant content (the deposited mass did not increased as C_{latex} was varied from 3 to 8 g l^{-1} (Fig. 6)).

4.2. Effect of surfactants

It should be recognised that latex dispersions are surfactant stabilised, and in order to obtain a given solid concentration the initial latex suspension was diluted with water: a high solid concentration was then associated with both a high ionic strength and a high surfactant content, and then with a high conductivity as shown in Fig. 6. This has rarely been recognised nor specified in previous works. The effect of ionic strength (approximately in the range 10^{-3}–10^{-2} M whatever C_{latex}) seemed negligible in our work, since no variations of zeta potential and deposit porosity were observed with increasing latex concentration. Consequently, the stabilisation of the deposited mass and the deposit thickness with increasing latex concentration is likely to be partially due to surfactant content: under high latex concentration, the surfactants accumulated in the deposit could enhance electrical repulsion with latex particles in the suspension (i.e. at the surfaces at which the surfactants are adsorbed). In the deposit, due to close contact of particles with each other, the interactions between surfactants adsorbed at the latex surface could be reinforced. This explanation may partially account for the increase in irreversible deposit observed at high latex concentration and the irreversible phenomena observed when filtering latex suspension using a membrane with a residual fouling ($R_{m'}$) due to internal fouling by surfactant adsorbed latex particles (Fig. 5b).

The surfactant content seems then responsible for modifications of deposit characteristics (stabilisation of deposited mass and deposit thickness; increase of irreversible deposit) and affects consequently the stability filtration zone (J_{crit} decreased when the surfactant content increased (Fig. 7)), which has been rarely reported in the literature.

5. Conclusions

The simultaneous determination of the critical permeation flux, J_{crit}, and deposit characteristics formed beyond the critical threshold under various operating conditions (pore diameter, crossflow velocity, latex concentration, surfactant content) made it possible to better understand crossflow filtration stability and reasons of filtration alterations. The critical parameter, J_{crit}/τ_w, defined the conditions required for no particles deposition and high stable filtration performance. This parameter was independent of the clean hydraulic resistance of the membrane and therefore of membrane pore size and was consequently more appropriate than $\Delta P_{crit}/\tau_w$ previously suggested in the literature to characterise the stability zone of a membrane separation. This work also pointed out that the latex suspension, even with a low size polydispersity, is a complex suspension containing large amount of surfactants. The surfactants were shown to affect both the deposit characteristics and J_{crit}, observations rarely reported in the literature.

Acknowledgements

The authors would particularly like to thank Chris Manning for technical assistance.

References

[1] J.A. Howell, Sub-critical flux operation of microfiltration, J. Membr. Sci. 107 (1995) 165–171.

[2] O. Le Berre, G. Daufin, Skimmilk crossflow microfiltration performance versus permeation flux to wall shear stress ratio, J. Membr. Sci. 117 (1996) 261–270.
[3] G. Gésan-Guiziou, E. Boyaval, G. Daufin, Critical stability conditions in crossflow microfiltration of skimmed milk: transition to irreversible deposition, J. Membr. Sci. 158 (1999) 211–222.
[4] H. Li, A.G. Fane, H.G.L. Coster, S. Vigneswaran, Direct observation of particle deposition on the membrane surface during crossflow microfiltration, J. Membr. Sci. 149 (1998) 83–97.
[5] P. Bacchin, P. Aimar, V. Sanchez, Model for colloidal fouling of membranes, AIChE J. 41 (2) (1995) 368–376.
[6] S.S. Madaeni, The effect of operating conditions on critical flux in membrane filtration of latexes, Trans. IChemE, Part B 75 (1997) 266–269.
[7] D. Wu, J.A. Howell, R.W. Field, Critical flux measurement for model colloids, J. Membr. Sci. 152 (1999) 89–98.
[8] R.W. O'Brien, L.R. White, Electrophoretic mobility of a spherical colloidal particle, J. Chem. Soc., Faraday Trans. II 74 (1978) 1607–1613.
[9] P. Harmant, P. Aimar, Coagulation of colloids retained by porous wall, AIChE J. 42 (12) (1996) 3523–3532.
[10] R.J. Wakeman, Visualisation of cake formation in crossflow microfiltration, Trans. IChemE, Part A 72 (1994) 530–540.
[11] T. Kawatatsu, M. Nakajima, S.I. Nakao, S. Kimura, Three-dimensional simulation of random packing and pore blocking phenomena during microfiltration, Desalination 101 (1995) 203–209.
[12] E. Fischer, J. Raasch, Model tests of the particule deposition at the filter medium in crossflow filtration, in: Proceedings of the World Filtration Conference, Ostend, 1986, pp. 11.11–11.17.
[13] S.S. Madaeni, A.G. Fane, D.A. Wiley, Factors influencing critical flux in membrane filtration of activated sludge, J. Chem. Technol. Biotechnol. 74 (1999) 539–543.
[14] B. Fradin, R.W. Field, Crossflow microfiltration of magnesium hydroxide suspensions: determination of critical fluxes, measurement and modelling of fouling, Sep. Purif. Technol. 16 (1999) 25–45.